SPARK TESTING IN THE IDENTIFICATION OF STAINLESS STEEL AND SUPERALLOY SCRAP

J. M. Larrain, W. D. Riley, and R. D. Brown, Jr.

U.S. Department of the Interior
Bureau of Mines
Avondale Research Center
Avondale, Maryland 20782-3393
USA

Summary

The Bureau of Mines is studying methods of identification of scrap that will lead to better segregation, conservation of strategic materials, and better utilization of existing resources. Spark testing--the visual examination of the spark stream generated when a metal is struck against a grinding wheel--has been used successfully for many years in the classification of alloy steels. Research using spectrophotometric methods to determine the characteristics of the light emitted by the sparks, and a minicomputer to recall and compare spark patterns is described. The utility of this instrumental method for the rapid identification of stainless steels and superalloys is discussed.

Introduction

One of the objectives of the Materials and Recycling Technology program of the United States Bureau of Mines is the conservation and reutilization of strategic metals. Proper identification, prior to sorting, is a critical factor in the recycling of metallic scrap. The Bureau of Mines has over the years devoted substantial efforts to its study and improvement (1-4).

Speed is of the essence in a practical identification method. For the most part, metallic scrap has a low value on a per-piece basis. This value is not always sufficient to cover the costs of whatever instrumentation may be used and the wages of the personnel doing the identification and sorting. Spark testing has been used for many years in the sorting of ferrous metals and alloys, where it has proved to be fast and reliable (5). It consists of the visual examination of the stream of sparks generated when applying a metal against a revolving abrasive wheel. Different alloying elements impart different characteristics to the spark stream--color, brightness, trajectories, and behavior of the incandescent particles.

The main shortcomings of traditional spark testing are the requirement of experienced personnel and its inability to identify unknown alloys, serving mainly as a comparison method (6). Its attractiveness is in its speed and the minimum sample preparation required. Apart from simple precautions to avoid cross-contamination, the method essentially creates its own fresh, clean surface. This work aims at automating this technique by substituting modern instrumentation for the trained observer in the hope that substantial improvements in sensitivity and selectivity may be realized.

This research is an extension of the work of Riley and Brown (7), who discovered that instrumental analysis of the spectral characteristics of the light emitted by the spark stream could be used for alloy identification, even in cases where the traditional (visual) spark testing was unsuccessful. In their exploratory study, Riley and coworkers (8) dealt with just a few alloys, and while utilizing several instruments, their main conclusion was obtained through the analysis of the sparks with a photodiode array optical spectrometer. The work reported here has more of a developmental character and, in recognition of the need to maintain low costs in any practical application of this technique, has concentrated on the use of filters combined with light detectors. Our objective has been the collection of information sufficient for the development of a reliable and inexpensive instrument for rapid identification based on the spark phenomena. The spectrometer used by Riley and coworkers (8) had sufficient resolution to show that there were no sharp discontinuities in the spectra, which appeared to have a mainly thermal origin. The method can not have the resolution and specificity inherent for instance in atomic emission spectroscopy.

In what follows we present descriptions of our methodology, equipment, and the results of our observations to date, both in general terms and as applied to the identification of stainless steel and superalloy scrap.

General

The light emitted by the spark stream generated while grinding a single sample is inherently variable. Recognition of this is essential to the proper selection of instrumentation and methodology. The photodiode array spectrometer used by Riley and coworkers (8) yielded time-averaged spectra over 0.5 s of exposure time. Some variability was evident, but much less than with the other two methods they tested: transmission filter-light detector combinations multiplexed to a single readout instrument, and a sequential (scanning) spectrometer.

Exploratory tests using light detectors with optical bandpass filters and a two-channel oscilloscope and photographic camera for display confirmed the contribution of the following factors to the variability of the spark pattern:

i) The variable number of spark streaks within the field of view of the light detectors used, owing to the quasi-random nature of spark generation during grinding, and their resulting spatial distribution. In the tests, a particular spark would remain within the view of the detectors for several milliseconds, depending on the acceptance angle of the optics, distance to the spark stream and speed of the incandescent particles. Particle speed depends on the peripheral speed of the abrasive wheel and the particular flow pattern of the air in the vicinity of the wheel.

ii) "Bursts," reportedly the disintegration of burning particles, cause rapid variations in light intensity, within milliseconds, caused by the sudden increase in radiating surface area. We have not reached definite conclusions regarding the spectral distribution of the light emitted during bursts, but we have indications of some spectral differences between periods of high and low overall light intensities.

iii) The spectral distribution changes with position in the spark stream; for steels the mean spark temperature reportedly rises and then decreases with increasing distance from the abrasive wheel (9). The spectral distribution is also affected by varying the pressure against the wheel or the grinding time; higher pressures or longer grinding times yield "hotter" sparks.

The simplest possible approach was taken in the present phase of the investigation. The light gathered at a representative location was analyzed as a function of wavelength and time, without attempting to isolate the different contributions to the observed behavior. As previously mentioned, the basic measurements involved analysis of the light with combination bandpass filters and light detectors. This is in some respects very similar to the spark temperature determinations of Riezler and Hardt for steels (9). The latter used two photomultipliers and interference filters centered at 601 and 797 nm along with a dual trace oscilloscope and photographic camera for data recording. They concentrated on spark temperatures, and did not consider application of their results to alloy identification.

Previous determinations at the U.S. Bureau of Mines (7,8) have covered for the most part the visible wavelength range. We have included here measurements in the near infrared, both in search of the most useful

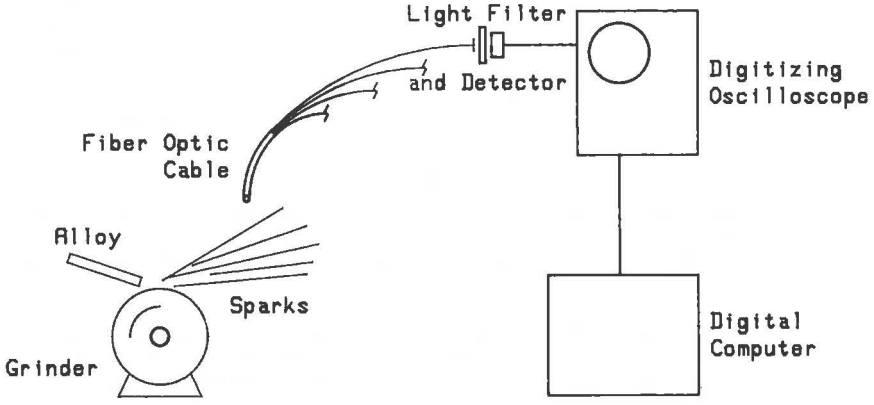

Figure 1. - Experimental system.

region of operation, and because of the higher sensitivity offered there by inexpensive sensors. Preliminary estimates, later confirmed in practice, were that the highest sensitivities in terms of electrical power developed at the sensor would be in the range 800-1,000 nm. These calculations were based on the sensitivity of commercial detectors, the transmission characteristics of fiber optic cable and glass, and were carried out for light of purely thermal origin at surmised spark temperatures.

Instrumentation

The system used in this investigation is shown schematically in figure 1. A bench grinder fitted with a 14.2 cm diameter medium grit aluminum oxide wheel (Dayton Electric Manufacturing Co. 5X594*) rotating at 3,450 rpm was used for the tests; no attempt was made at optimizing the abrasive parameters (pressure, angle, etc.). Light from the spark stream enters a fiber optic cable which divides into four separate strands leading to individual bandpass filters followed by light detectors (Oriel Corp. 7180 photovoltaic detectors). Characteristics of the interference filters used, procured from Oriel Corporation, are listed in table I. A violet filter, with transmission centered at 405 nm, was tried, but for most alloys of interest the light output within this color band was so low as to make the measurements unusable.

*Mention of specific brand names is made for identification purposes only, and does not imply endorsement by the U.S. Bureau of Mines.

TABLE I. - Characteristics of bandpass filters used.

Supplier Model	Peak Transmission, pct	Peak Wavelength, nm	Bandwidth (50 pct peak) nm	Spectral Region
5757	73	542	71	Green
5763	54	705	60	Red
5769	72	842	74	Infrared
5775	69	1,001	83	Infrared

The light detectors are connected directly to a 4-channel digitizing oscilloscope (Tektronix Inc. 5223 with 5B25N time base and two 5A26 dual differential amplifiers modified for high input impedance) used in fully differential mode with DC coupling. The oscilloscope communicates with a digital computer system (Hewlett-Packard 9816 and associated peripherals), allowing convenient collection of data, transfer of the oscilloscope readings to flexible diskettes for storage, and subsequent data reduction and analysis.

Proper selection and alignment of the optical components required special care. The light under observation is emitted by a multitude of sources moving at high speed, and it is difficult under these circumstances to have light of identical qualities impinge simultaneously on all the filter-detector combinations. Typically, we could observe light from the same source reaching the detectors at different times, or attenuated differently, depending on the relative position of the light source and the system optics. The randomness inherent in the fiber optic cable used proved insufficient by itself. With unprepared ends, each fiber selectively collects light from a certain portion of space (the acceptance cone), giving rise to fiber-to-fiber variations with the movement of the light sources, of sufficient magnitude to be detected. Masking, so as to have the optics see only a limited portion of the spark stream was unsuccessful; movement of the shadows cast by the mask made matters somewhat worse.

These effects were minimized by two approaches, which had the unavoidable side effect of attenuating the overall light levels available at the detectors. First, increasing the separation between the detectors and cable ends decreases the effects of individual fibers and possible nonuniformities of detector active areas. Average separations used are 0.23 cm between cable end and front filter surface, and 0.83 cm between back filter surface and detector active area. Second, the light sources were made more diffuse in character by interposing between the fiber optic cable and the spark stream a short section of glass rod (0.9 cm long by 0.9 cm diameter) with both ends ground to a translucent state, at a distance of 0.64 cm from the cable end.

Operating Procedure

Operation was in a darkened room, with light levels below the limits of detection of the system, and with the spark stream against a black

matte background. As recommended in the literature, the grinding wheel was dressed when changing alloys to avoid confounding of results from residues of prior measurements.

For most alloys, light was collected from a position facing the spark stream, 15 cm away from the side of the wheel. When the spark streams are short and emit little light (as in superalloys) the end of the fiber optic cable was placed next to the wheel, about 2 cm away from the sparks.

The different oscilloscope parameters would be selected under prompting by the digital computer system. Some experimentation is required for the gain setting of each channel because of the changeable signal strengths. The measurements reported here required full scale settings of 0.5 mV to 50 mV. Sweep times were uniformly 50 ms. This time span offered a reasonable compromise between the requisite detail in the representation of the spark phenomena, and length for the measurements to be representative.

The oscilloscope would then take one set of measurements, without sparking, as zero reference for each channel, and proceed to the readings on the spark stream. Both free-running and level-triggered sweep modes were used with little operational difference. The metal specimens were applied momentarily to the grinding wheel, in bursts, to minimize the bulk heating of the samples. Before accepting the data, the digital computer system checked that reasonable voltage levels were present and that maximum ranges had not been exceeded. Measurements done with little or no light, or too much light, were automatically rejected. The measurements continued until data for 5 sweeps were collected. The overall process, including the transmission of data between the oscilloscope and the digital computer system would take one or two minutes for properly set parameters.

Thin specimens presented an additional difficulty. It is fairly easy to raise a portion of them to incandescence, usually along the thin edge facing the spark stream. Because of their relative areas, the light emitted by this incandescent region can be much more intense than that emitted by the spark stream, and can mask the phenomena under investigation. Because of the location where light was collected, this effect was more evident with superalloy specimens. Data from runs that were influenced by this effect were discarded.

Data Reduction

The data were processed in two stages. They were first corrected for the characteristics of the measuring system, and then were converted to a form expected to be more useful from the point of view of alloy identification. Data reduction to date has concentrated on the description of time-averaged spectral spark properties, as probably the least expensive way to implement the concepts in a practical field instrument.

Each oscilloscope sweep produced, from each light detector, 508 voltage readings with resolutions of 0.1 pct of full scale ("10 bits"). Because of the switching procedure of the oscilloscope used, these

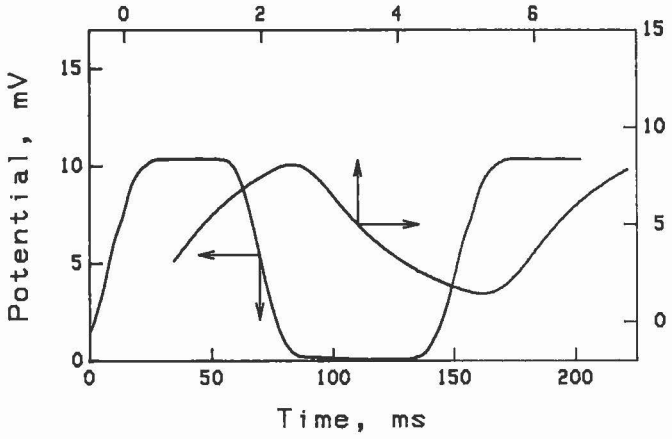

Figure 2. - Effect of signal rate of change on the measured potential.

readings were not evenly spaced in time, being taken in groups of two readings in adjacent intervals of a 4-interval basic timing cycle. Furthermore, we found the relative channel to channel timing information furnished by the oscilloscope to be in error; fortunately a separate detailed study of its triggering sequences was able to unequivocally resolve the timing relationships for the unit employed. Five hundred and four evenly spaced values in precise time coincidence for each of the light detectors were obtained with the following procedure: One-half of the readings from each detector were used directly, those that were taken at desired times. The timing was off for every other reading, and in their stead, values calculated by parabolic interpolation through the three determinations nearest the desired times were adopted. No difficulties were experienced; the sweep speeds (corresponding to 10,000 readings/sec for each detector) were sufficiently fast to avoid discontinuities and to allow valid interpolation between readings.

Analysis of the dynamic response of the system to light showed that rapidly varying signals were attenuated relative to more slowly changing ones. Figure 2 shows this effect for a light detector receiving the same radiation, but varying at different rates. (Arrows indicate which scales are appropriate.) The curves were obtained by interposing rotating vanes between a constant light source and the detector, and changing the rotational speed. Compensation for this was required because slight differences in the system components caused different relative attenuations of the signals from the light detectors, which was quite noticeable at the

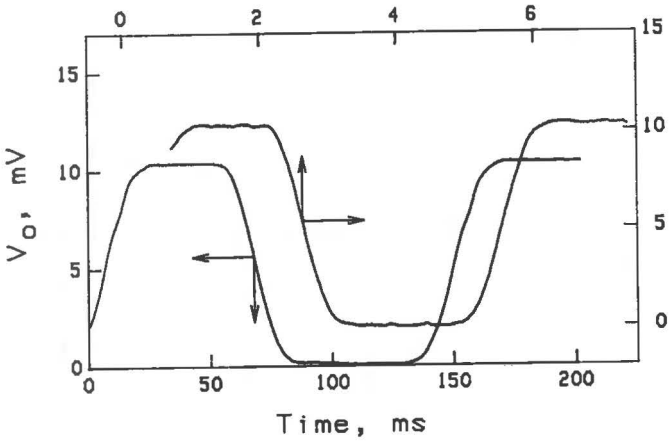

Figure 3. - Attenuation correction for signals in Figure 2 with τ = 1.36 ms.

high data collection rates used. The following expression was found to describe very satisfactorily this effect:

$$V_o = V + \tau \frac{dV}{dt} \qquad (1)$$

where V is the measured potential, V_o the electromotive force developed at the light detector (function only of the instantaneous light intensity), t the time, and τ a constant. This equation has the same form as the attenuation due to a filter consisting of a resistance (R) and capacitance (C) connected to an ideal detector, with time constant τ equal to the product R x C. Values of the constants τ ranging from 1.28 to 1.52 ms for the four detector circuits were obtained by fitting the measurements performed with the rotating vanes. As an example, figure 3 shows V_o calculated from the data in figure 2 using τ = 1.36 ms; the two curves would almost perfectly coincide upon superposition.

Two methods of compensation for this filter effect were developed. The first involves using equation (1) and evaluating the light-dependent quantity V_o. The only drawback of this procedure is in the uncertainties introduced by the numerical evaluation of the time derivative, which make necessary the use of smoothing techniques. It was found that satisfactory results could be obtained by approximating this derivative by the slope of the least squares straight line passing through the point of interest, the 8 determinations prior to it, and the 8 determinations following it. It turns out, however, that when studying the time-averaged

quantities that are the subject of this report, V_o is not really necessary, and equivalent information is obtained by just reducing all the determinations to a common value of τ--in other words, correcting the signals so they appear to have passed through identical filters. The measurements reported here are all referred to a time constant equal to the largest value determined--1.52 ms--so as to avoid introduction of random variations by (in effect) differentiation, or undue smoothing.

The corrections were based on the following form of equation 1:

$$V^* + \tau^* \frac{dV^*}{dt} = V + \tau \frac{dV}{dt} \tag{2}$$

where V^* are corrected values, referred to the time constant τ^*, and the other terms have their earlier meaning. The solution to this equation can be put in the following form:

$$V^* = Ae^{-t/\tau^*} + V - (1 - \tau/\tau^*)e^{-t/\tau^*} \int_o^t e^{t/\tau^*} \frac{dV}{dt}\, dt \tag{3}$$

where A is an arbitrary constant, taken as zero. Integration with respect to V instead of t using the trapezoidal rule approximation allows the derivation of the following relationships giving the corrected values V^* at successive times:

$$I(0) = 0 \tag{4}$$

$$I(t + \Delta t) = e^{-\Delta t/\tau^*} I(t) + \frac{1}{2}\left(1 + e^{-\Delta t/\tau^*}\right)\left[V(t+\Delta t) - V(t)\right] \tag{5}$$

$$V^*(t) = V(t) - (1 - \tau/\tau^*)\, I(t) \tag{6}$$

Circuit modifications (for example, the incorporation of capacitors) were also found effective in detector matching; the numerical correction procedure was preferred, however, because of the flexibility offered.

Finally, the light detectors used do not have a perfectly linear response in terms of developed electromotive force as a function of incident radiation energy. In our experience, they are more sensitive at low light levels and exhibit saturation effects at high levels. The detectors were calibrated (with the associated filters in place) by comparison of their response to the square of the reciprocal of the distance from the entrance of the fiber optic cable to a light source of constant output. A more absolute calibration was obtained by taking readings on radiation from a furnace enclosure at 1,000° C.

Again, for the purposes of the time-averaged quantities to be dealt with in this report, the order in which the corrections for detector

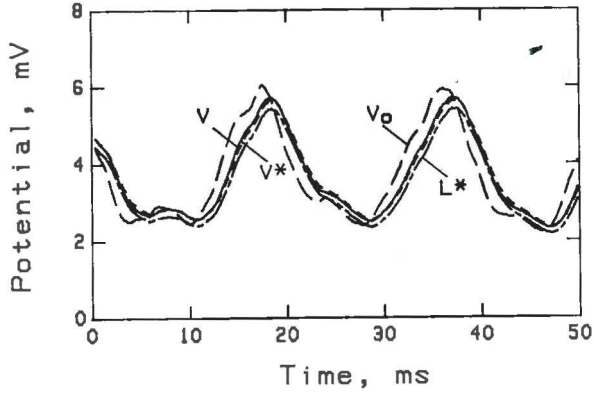

Figure 4. - Typical corrections to the measured potential V. L^* denotes the correction of V^* for detector nonlinearity.

non-linearity and the attenuation effect are carried out is immaterial. To a good degree of approximation, the linearized values of attenuated voltages are equal to attenuated values of linearized voltages. The corrections were uniformly applied in the order described. They are small (a few percent) as evidenced in figure 4, which shows a representative measurement (medium carbon steel sparked, 705 nm filter, τ = 1.28 ms, τ^* = 1.52 ms) and corresponding corrections including the calculation of the light-dependent electromotive force V_o.

Further manipulation of the data involves their representation in a fashion meaningful for correlation purposes, and the development of a possible alloy identification method. Several avenues are open at this stage. After compensation for the variability in the overall light emitted by the spark stream, the data effectively reduced to the ratios of the intensity measurements at the different wavelengths--these ratios embody the spectral characteristics of the radiation.

We have elected to express the findings in terms of apparent source (spark stream) temperatures that can be obtained from the experimental data. The fundamental assumption in the calculations is that the radiation is gray-body type, at least approximately.

After linearization, the voltage V_i developed at the detector "i" receiving light of wavelength λ_i from a gray body at temperature $\overline{T}$ is given by:

$$V_i = \frac{K_i \overline{V}}{e^{C_2/\lambda_i \overline{T}}} \qquad (7)$$

where K_i is a characteristic constant for each detector-filter combination, $\overline{V}$ is a factor compensating principally for the instantaneous overall light level (as seen by all the detectors), and $C_2 = 0.01439$ m•K is a fundamental constant. In all rigor, a value of 1 should have been substracted from the denominator in equation 7; however, for the present conditions, this term is negligible in comparison with the exponential, and its omission significantly simplifies the treatment.

Readings from two detectors are required to obtain $\overline{T}$ and $\overline{V}$ from equation 7. A least squares procedure was used to obtain $\overline{T}$ and $\overline{V}$ from readings from more than two detectors. It consists of using the right hand side of equation 7 to define calculated values of the voltages V_i and finding the values of $\overline{T}$ and $\overline{V}$ that minimize the sum of the squares of the logarithms of the ratios between the calculated and experimental voltages. Solution to the resulting system of equations is straightforward:

$$\frac{C_2}{\overline{T}} = \frac{\sum\lambda_i^{-1}\sum\ln(V_i/K_i) - n\sum\lambda_i^{-1}\ln(V_i/K_i)}{n\sum\lambda_i^{-2} - (\sum\lambda_i^{-1})^2} \tag{8}$$

$$\ln\overline{V} = \frac{\sum\lambda_i^{-2}\sum\ln(V_i/K_i) - \sum\lambda_i^{-1}\sum\lambda_i^{-1}\ln(V_i/K_i)}{n\sum\lambda_i^{-2} - (\sum\lambda_i^{-1})^2} \tag{9}$$

where n is the number of detectors, and the summations are carried out over all the detectors.

Instantaneous values of apparent spark stream temperatures were obtained with equation 8 at the times for which simultaneous readings from the light detectors were available. Figure 5 shows results for one such run, which incorporates the data in figure 4, and uses readings from only three of the detectors. Values λ_i corresponding to the transmission peaks listed in table I were used in all the calculations.

Regarding the constants K_i, they were at first estimated by taking measurements on radiation from a furnace enclosure at a known temperature. A simpler and more practical calibration procedure was adopted, consisting of using the radiation from the sparking of a known alloy. Based on the preliminary estimates, a value of 1,667 K was adopted for the time average apparent temperature of the sparks from a medium carbon steel sample. All measurements were referred to this value by including this alloy in any series of readings, and selecting the constants K_i accordingly. Conversion to any other reference can be effected with equation 7.

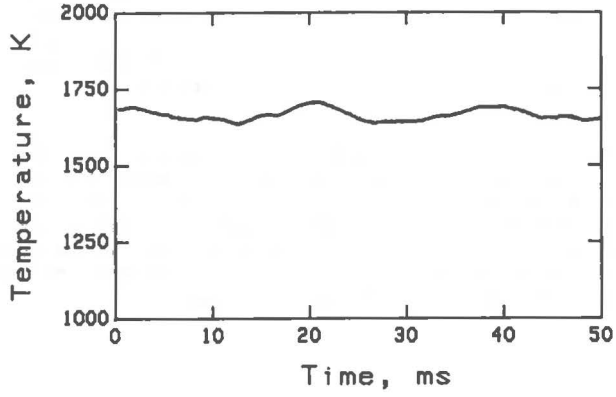

Figure 5. - Typical apparent spark temperatures. Incorporates data in Figure 4.

Results

For many alloys, the calculated apparent spark temperatures are surprisingly constant in spite of the wide and rapid variations in intensity of the light emitted by the stream (figures 4 and 5). These temperatures appear to be characteristic of the metals sparked, and their time averages are natural parameters for a metal identification scheme.

Results to date are summarized in table II. The time averages listed were obtained numerically from the instantaneous values; data for all the oscilloscope sweeps were combined.

It should perhaps be stressed at this point that apparent source temperatures are employed here mainly for their usefulness in placing the findings in perspective. The discussion could equally well be addressed to intensity ratios, and in fact any practical instrumentation would probably be based directly on these ratios, avoiding the complexities of conversion to temperature. In any case, there is a simple relationship between temperature and relative light intensities: Equation 8 gives the slope of the least squares straight line relating the natural logarithms of the linearized voltages to the reciprocals of the radiation wavelengths. Constancy in apparent temperature is just a manifestation of constancy of overall spectral characteristics.

Table II reflects a desire to minimize the number of detectors. The bulk of the figures in the table are based on the readings from just 3 detectors--not coincidentally, at the longer wavelengths, that yield the strongest signals. Only the last column includes information from the fourth detector, at 542 nm. The values listed should not be considered absolute, as they are system dependent. For many reasons, spark radiation is not strictly gray-body and different apparent temperatures $\overline{T}$ are

TABLE II. - Results. Time averaged values.

	Observations at 705, 842, and 1,001 nm				Four detectors
			Standard Error		
Metal	$\bar{T}$, K[1]	$\bar{D}$[2]	of $\bar{T}$, K	of $\bar{D}$	$\bar{T}$, K
Udimet 500	1191	-.002	16	.018	1284
Haynes 188	1193	-.009	27	.029	1283
Inconel 600	1197	.023	30	.023	1282
Inconel 625	1201	.016	26	.023	1301
Hayes 25	1211	-.035	29	.014	1281
Hastelloy G	1213	.008	21	.022	1283
Hastelloy B-2	1220	-.033	14	.015	1276
Hastelloy C-276	1222	-.039	17	.024	1319
Rene 41	1223	.012	26	.038	1339
B-1900	1234	-.017	20	.027	1288
Incoloy 800	1264	.019	63	.029	1364
M2 Tool Steel, Sample 1	1369	-.007	19	.008	1388
M2 Tool Steel, Sample 2	1372	-.011	13	.008	1389
M2 Tool Steel, Sample 3	1381	-.009	15	.007	1394
Greek Ascoloy	1559	-.011	11	.007	1553
Stainless Steel 316	1620	-.007	18	.008	1614
Stinless Steel 430	1628	.008	34	.024	1629
Stainless Steel 304	1631	.001	25	.014	1635
Stainless Steel 301	1641	-.004	19	.009	1635
ARMCO Iron	1649	.014	16	.012	1677
Stainless Steel 201	1658	-.008	17	.008	1645
MIL-S-17758 Mn Steel	1659	.017	20	.007	1666
Medium Carbon Steel	1667	0.000	20	.009	1667
Ti-6 Al-4 V	2144	.019	56	.019	2122

[1] $\bar{T}$, average spark temperature.

[2] $\bar{D}$, a measure of the departure from gray-body radiation. See text.

obtained depending on the spectral bands used and system geometry. As illustration, consider the different apparent spark temperatures obtained from 3 and 4 detectors, as listed in the first and last columns of table II, in spite of using identical references.

Table II agrees with our intuitive impression of spark temperatures, being lower for superalloys and higher for ferrous metals and titanium alloys. Uncertainties are illustrated by the 3 tool steel samples. Regarding the values themselves, we can only speculate about their absolute accuracies or interpretation. Some of them, in particular for stainless steels, appeared at first to be too high. But examination of swarf from the grinding of stainless steel 316 revealed the presence of a few globules of metal that had clearly undergone melting; temperatures surpassing the softening points of these alloys are indeed possible in the process.

Inspection of the apparent temperatures in table II, reveals that they are probably sufficient to separate alloys into broad classes--superalloys, tool steels, stainless steels--but this parameter does not allow discrimination between the many alloys yielding close readings. Perhaps we should comment here that just separation into alloy groups by a fairly simple instrument may by itself be of great practical value.

On the subject of relative measurement reliability, apparent temperature differences of 10 K or higher are believed to be meaningful, at least in side-by-side comparisons, or with appropriate calibration. Stainless steel 304, for instance, consistently yielded higher values than 316, irrespective of the calibration method selected. These alloys are practically indistinguishable by traditional (visual) spark testing.

Resolution of the overlaps requires additional information. The discussion that follows concentrates on the use of only 3 detectors; more detectors simplify the task. Inspection of table II, for instance, reveals that some of the overlaps can be resolved simply by consideration of $\overline{T}$ calculated with data from 3 and 4 detectors, as illustrated by Inconels 600 and 625, and the separation of stainless steel 201 and the manganese steel specimen.

Readings from 3 detectors can furnish only one more independent quantity, and we selected for scrutiny the departure of the radiation from gray-body type. A measure of this departure is the ratio between voltages calculated with equation 7 and the experimental ones. $\overline{D}$ in table II denotes the time average of the natural logarithm of this ratio for the mid-frequency detector, at 842 nm. Differences in $\overline{D}$ of about 0.007 or larger are believed significant and could be used to distinguish between for instance Haynes 188 and Inconel 600, stainless steel 316 and 430, Hastelloys G and B-2. The questions of accuracy or precision of this parameter, and that of $\overline{T}$, are addressed in the next section, describing the present direction of our research.

Work in Progress

We are convinced of the effectiveness of instrumenting spark testing, and are well satisfied with the results to date. Instrumentation of spark testing does not just look promising. It can be useful in many practical situations, in particular, those involving stainless steels and superalloys.

Work in progress is directed towards making alloy identification unequivocal, by better delineating the technical limitations, simplification of the instrumentation, and perhaps uncovering more appropriate parameters to base the instruments on.

A case in point is that of precision of the values in table II. We have already mentioned our views on the reliability of the average values of $\overline{T}$ and $\overline{D}$. The standard errors listed (root mean square deviations from the average) for $\overline{T}$ and $\overline{D}$ in table 2 have more to do with variations characteristic of the spark stream than random measurement or instrumentation errors. Variations in spark characteristics for the

different alloys are not entirely random--they depend on the grinding rates, the number of spark streaks within the field of view of the instrument, and the number and relative intensity of bursts. These are now dynamic characteristics, and we are studying their quantification, and their usefulness from the point of view of alloy identification. Very preliminary data seem to indicate that the standard errors in $\overline{T}$ and $\overline{D}$ are, themselves, characteristic of the alloys sparked (and system geometry) and could be used as part of the identification procedure.

References

1. Maynard, A.W. and H.S. Caldwell, Jr., "Identification and Sorting of Nonferrous Scrap Metals", Proceedings of the Third Mineral Waste Utilization Symposium, U.S. Bureau of Mines and IIT Research Institute, Chicago, March 14-16, 1972, pp. 255-64.

2. Newell, R., R.E. Brown, D.M. Soboroff, and H.V. Makar, "A Review of Methods for Identifying Scrap Metals", U.S.B.M. IC 8209, 1982.

3. Riley, W.D., R.E. Brown and D.M. Soboroff, "Rapid Identification and Sorting of Scrap Metals," Conservation and Recycling 6(4), pp. 181-92, 1983.

4. Brown, R.D., Jr., W.D. Riley and C.A. Zieba, "Rapid Identification of Stainless Steel and Superalloy Scrap", U.S.B.M. RI 8858, 1984.

5. "Metals Handbook", 1939 edition, American Society for Metals, Cleveland, 1939.

6. Buzzard, R.W., "The Utility of the Spark Test as Applied to Commercial Steels", Research Paper RP 605, Bureau of Standards Journal of Research 11, pp. 527-40, 1933.

7. Riley, W.D. and R.D. Brown, Jr., "Device and Technique for Scrap Metal Spark Pattern Recognition", U.S. Patent Application 623753, June 26, 1984.

8. Riley, W.D., B.W. Dunning, Jr., and D.M. Soboroff, "Spectral Characteristics of Grinding Sparks Used for Identification of Scrap Metals," U.S.B.M. RI 8932, 1985.

9. Riezler, W. and L. Hardt, "Temperature Measurement on Grinding Sparks," Z. Angew. Phys. 6, pp. 497-9, 1954.